Sborník vědeckých prací Vysoké školy báňské - Technické univerzity Ostrava
řada stavební, ročník 15, číslo 2, rok 2015
článek č. 6

Filip HOKEŠ[1]

SELECTED ASPECTS OF MODELLING OF NON-LINEAR BEHAVIOUR OF CONCRETE DURING TENSILE TEST USING MULTIPLAS LIBRARY

Abstract

The subject of this paper is to describe some of the aspects manifesting in the use of the elasto-plastic material model library multiPlas, which was developed to support non-linear computations in the ANSYS system. The text focuses on the analysis of numerical simulations of a virtual tension test in several case studies, thereby the text endeavours to describe the problems connected with modelling non-linear behaviour of concrete in a tensile area.

Keywords

Concrete, fracture mechanics, damage theory, material non-linearity, Menétrey-Willam, FEM, ANSYS, multiPlas.

1 INTRODUCTION

The application of a non-linear description of the construction material behaviour at numerical simulations represents bringing mathematical modelling methods nearer to the real actions of structures. The finite element method (FEM), which is implemented to a number of commercial and academic software products (e.g. ANSYS [1], Atena [2]), is currently widely used for numerical simulations calculating on an effect of material as well as geometric non-linearity. Examples of applications of robust computational systems based on the finite elements for solving material non-linear problems are documented in a publication [3]. Other publications in professional journals and conference paper proceedings [4,5,6] are an evidence that the area of the description of quasi-brittle material structure behaviour in particular is a sphere of interest of many scientific workplaces and at the same time the mentioned points at issue have not been fully concluded so far.

One of the crucial problems of the constitutive relation definition for the concrete is the different behaviour under the tensile and compressive stress. The main difference lies in different proportions of the compressive and tensile strength that reaches significantly lower values. Considering the mentioned differences in concrete structure behaviour under different loads, the points at issue of the description of non-linear quasi-brittle material behaviour is connected with several theoretical areas: the theory of plasticity, the theory of linear and non-linear fracture mechanics and the damage theory [7]. This concept of so-called multi-surface plasticity is the essence of the material models in the multiPlas library [8] that was created as a supportive database for material non-linear computations in the ANSYS computational system. The level of the robustness of the mentioned combination of computational tools enables to solve a really varied scale of non-linear problems, but still some specific consequences can arise at these simulations caused by the application of the finite element method and assumptions of the applied theories. The dependence to the finite elements size (spurious mesh sensitivity), problems of strain localization and the idealization of boundary conditions can be included among these negative aspects. Even though the

[1] Ing. Filip Hokeš, Institute of Structural Mechanics, Faculty of Civil Engineering, Brno University of Technology, Veveří 331/95, 602 00 Brno, Czech Republic, phone: (+420) 597 148 207, e-mail: hokes.f@fce.vutbr.cz.

mentioned tools have the means intended for elimination of these defects, we can meet with their incorrect functionality in some cases.

The existence of often a large class of physically-mechanical and empirical parameters whose values are not systematized creates a significant problem connected with the application of the non-linear material models for the concrete, but also for other materials. Some of these parameters even do not have the physics and serve for instance as a stabilizing agent of the solution. One of the possibilities how to determine given parameters is the application of inverse identification methods among which exercises of artificial neural networks and optimization techniques can be included. However, the application of these methods requires a deep knowledge of the non-linear solution problems, the stability and the robustness of the solver as well as securing as smooth convergence as possible. The task of the presented text is to explain the aspects occurring at the solution of the material non-linear problems with the aid of the multiPlas library through several partial case studies whose successful solution has the potential to help at further applications of this material models library.

2 PROBLEM DEFINITION

To demonstrate the selected aspects occurring at the numerical investigation of the non-linear behaviour of the concrete, an elementary problem of the simple tension representing a virtual tension test on a concrete sample was chosen. The concrete sample of the C20/25 class in a shape of a beam of nominal dimensions: length l = 200 mm; height h = 100 mm; width b = 100 mm was considered for these purposes. This sample was exposed to tensile load on the opposites sides of the dimensions 100 x 100 mm. The form of the intended sample and the load scheme can be seen in Fig.1.

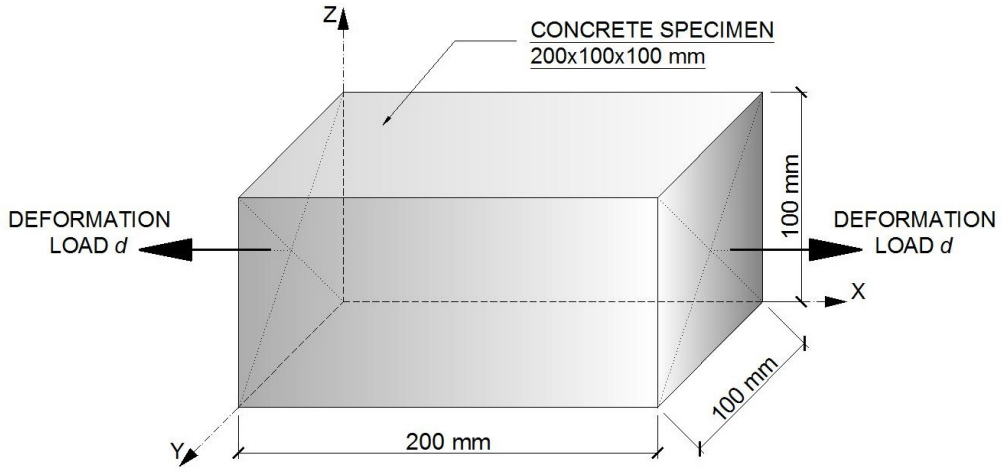

Fig. 1: Load scheme

The given task type was chosen with respect to its simplicity and the possibility to apply analytical methods to verify the results obtained by the non-linear solution with the use of the adequate material models. The dimensions of the considered sample further enabled to check a possible occurrence of the negative relation of the solution on the size of the finite element mesh. The selected type of the task also enabled to carry out computations at different levels of the complexness using both 3-D SOLID185 eight-node elements and plane PLANE182 four-node elements for the problems of the plane state of stress.

As for the load, the deformation load that appears to be more stable and better to converge at the computational solution was considered. The total load size was d_{tot} = 0.0001 m. During the virtual tension test it was considered as the horizontal displacement of a half size of d = 0.00005 m at the both ends of the body. On the basis of the elementary knowledge of the task and material geometry, a very simple analytic solution was carried out, whose purpose was to verify the subsequent numerical simulations. The above-mentioned values of the horizontal final deformations were with regard to the defect of a descending branch of the work diagram approximately 10 times greater than the deformation at reaching the material ultimate strength.

2.1 Simplified Analytic Solution

The simplified analytic solution was carried out under the assumptions of the linear elasticity theory. The purpose of the given solution was to determine the size of the introduced deformation $d_{lin,\max}$ at reaching the material tensile strength $\sigma_{t,\max}$ for which the following relation applies:

$$d_{lin,\max} = \frac{l \cdot \sigma_{t,\max}}{E_c} \tag{1}$$

where:

E_c – is the Young's modulus of elasticity [Pa],

l – is the length of the considered sample [m],

$\sigma_{t,max}$ – is the ultimate tensile strength [Pa]

Considering the fact that this was a testing study the value of the modulus of elasticity and the concrete tensile strength was taken from the existing Czech technical standard ČSN EN 1992-1-1 [9]. For the considered C20/25 concrete class the normative value E_c = 30 GPa was applied and the tensile strength value was considered of the proportions of $\sigma_{t,max}$ = 2.4 MPa. By substituting into the equation (1) the value of the tensile deformation at reaching the material ultimate strength was thus gained:

$$d_{lin,\max} = \frac{l \cdot \sigma_{t,\max}}{E_c} = \frac{0.2 \cdot 2.4 \cdot 10^6}{30 \cdot 10^9} = 1.6 \cdot 10^{-5} \text{ m} \tag{2}$$

On the basis of the determined deformation $d_{lin,\max}$ the maximum intensity of the tensile force $F_{t,\max}$ for the given tensile deformation load d_{tot} was determined. The following equation was applied for the computation of the tensile force:

$$F_{t,\max} = \frac{d_{lin,\max} \cdot E_c \cdot A}{l} = \sigma_{t,\max} \cdot A \tag{3}$$

After adjustment and substitution to the equation (3) the value of the maximum tensile force $F_{t,\max}$ was determined:

$$F_{t,\max} = \frac{d_{lin,\max} \cdot E_c \cdot A}{l} = \sigma_{t,\max} \cdot A = \sigma_{t,\max} \cdot b \cdot h = 2.4 \cdot 10^6 \cdot 0.1 \cdot 0.1 = 2.4 \cdot 10^4 \text{ N} \tag{4}$$

All the above-mentioned and calculated basic values of the *F-d* diagram of the load test are schematically indicated in the graph - see Fig. 2.

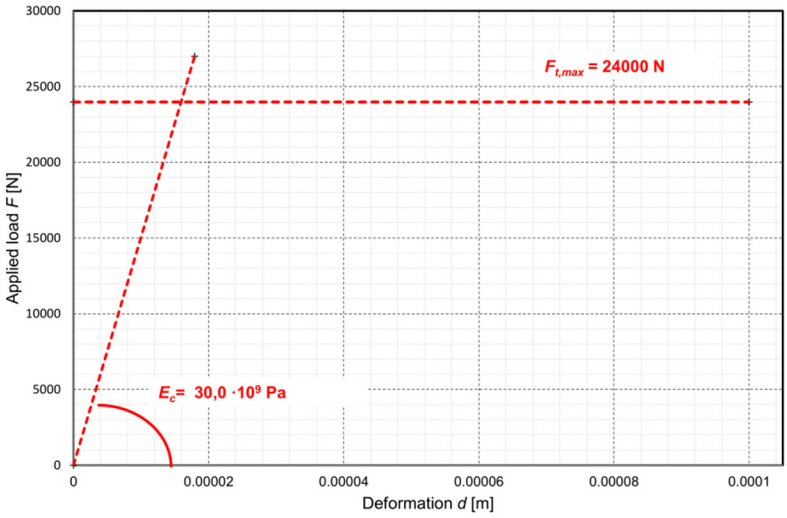

Fig. 2: Basic values of the *F-d* diagram of the load test

3 NON-LINEAR NUMERICAL ANALYSIS AND ITS SPECIFIC ASPECTS

For the virtual load test, which has been dealt with in the previous paragraphs, 4 sets of non-linear numerical simulations in total were carried out in the ANSYS computational system. The non-linear Menétrey-Willam material model from the multiPlas library was applied in all the cases. The effect of idealization of boundary conditions, the effect of the finite element mesh size, and the effect of a setting of some internal variables at the level of a final element was monitored within these case studies executed in the 2-D (3 sets) and in the 3-D environment (1 set).

3.1 Computational Model Geometry

The computational model creation including the setting of the material model, the application of boundary conditions, the setting and initialization of the solver and finally also the export of the resulting data indispensable for the *F-d* diagram creation were always performed within 1 programmed batch. The computational model geometry itself was with respect to its simplicity created in a hierarchical manner from points through the lines to the surfaces within the mentioned batch. In case of the 3-D alternative with the final elements of the brick type the above-mentioned surfaces were extruded in addition and thanks to this the body of the given size was created. The resulting geometric object was subsequently covered with the finite element mesh with the appropriate length of the side as can be seen in the examples in Fig.3.

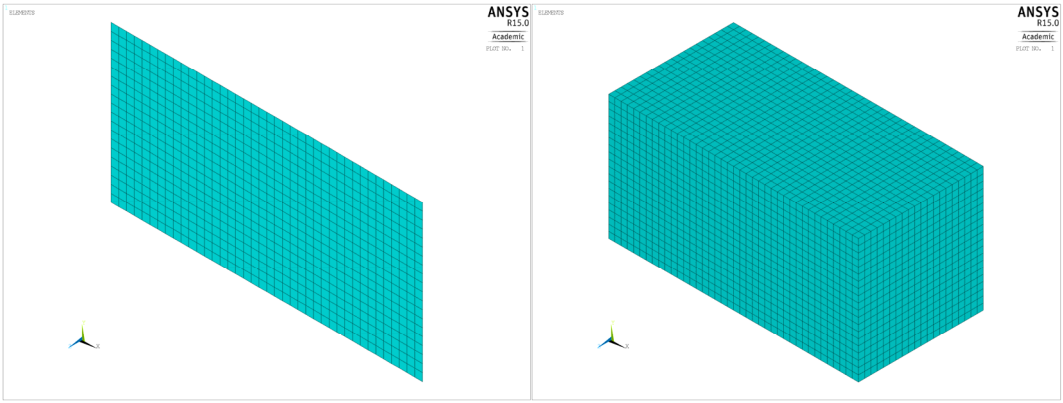

Fig. 3: Computational models with the mesh from PLANE182 and SOLID185 elements (element size – 5 mm)

The following cases of the finite element mesh dimensions were considered within the executed studies: 1 mm, 2 mm, 5 mm, 10 mm and 20 mm. However, this planning failed to be kept rigorously, as the requirements on the computational time in the case of the 1 mm alternative with the SOLID185 elements were enormous.

3.2 Material Model Description and Setting

The applied non-linear Menétrey-Willam [10] material model is based on the Willam-Warnke [11] yield surface, which is contrary to the Drucker-Prager surface the function of not only the first and the second, but also of the third invariant of the stress deviator (so-called Lode angle). Softening the corners of the deviatoric planes of the yield surface that, moreover, do not have a constant distance from the hydrostatic axis in the Haigh-Westergaard space [8] is achieved by this adjustment. This aspect is one of the basic characteristic features of the multi-surface plasticity concept that is currently applied at the multiPlas library models. Comparison of the deviatoric planes of the yield surface is shown in Fig. 4.

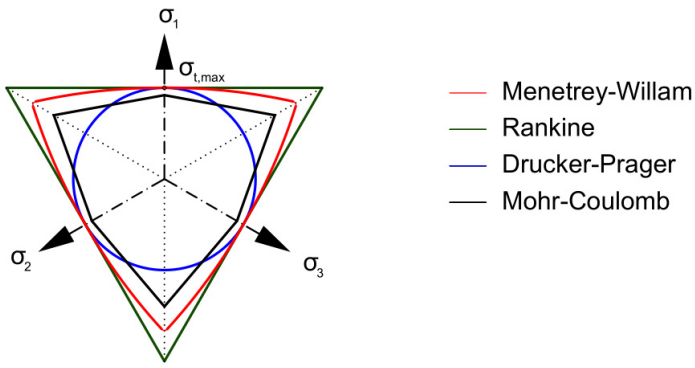

Fig. 4: Comparison of the deviatoric planes of the yield surface

The Menétrey-Willam material model belongs to a group of models that cannot cover the effect of strain rate on the state of stress. Irreversible strains arise at reaching the yield surface, while the disintegration of the total strain vector $\boldsymbol{\varepsilon}_{tot}$ into an elastic $\boldsymbol{\varepsilon}_{el}$ and plastic $\boldsymbol{\varepsilon}_{pl}$ part [8] is assumed.

$$\boldsymbol{\varepsilon}_{tot} = \boldsymbol{\varepsilon}_{el} + \boldsymbol{\varepsilon}_{pl} \tag{3}$$

From the point of view of the finite element method application the selected material model uses the smeared cracks concept. To solve the given problem an alternative using the softening function based on the dissipation of the specific fracture energy G_f was selected. In relation to the necessity to eliminate the negative relation of the solution on the size of the finite element mesh the non-linear Menétrey-Willam model uses Bažant's Crack Band concept [12].

To achieve corresponding non-linear functioning of this model, 10 material parameters in total whose description and values selected in the case studies are summarized in Table 1 need to be pre-defined. These parameters were chosen purely at random for the purpose of the simplicity of the executed study and thus do not have any connection to the actual parameters of the selected material. Their actual values could be obtained using the inverse identification method from the data originating from the real experiments, as indicated in the introductory passage.

Besides the above-mentioned non-linear parameters, linear-elastic parameters were necessary to be preset as well as required by the ANSYS computational system. With regard to this fact, the modulus of elasticity of the size of E_c = 30 GPa and the Poisson's ratio υ = 0.2 were set. In addition to these parameters having the character of the physically-mechanical qualities of the used material, also other state and computational variable whose detailed description can be found in the quoted literature [8] had to be preset.

Tab. 1: Material parameters – description and values selected in the case studies

Parameter	Unit	Value	Description
$\sigma_{c,\max}$	[Pa]	$30.0 \cdot 10^6$	Uniaxial ultimate compressive strength
$\sigma_{t,\max}$	[Pa]	$2.4 \cdot 10^6$	Uniaxial ultimate tensile strength
σ_b	[Pa]	$36.0 \cdot 10^6$	Biaxial compressive strength
Ψ	[°]	10.0	Dilatancy angle
κ_{cm}	[-]	$3.0 \cdot 10^{-4}$	Plastic strain corresponding to the maximum load
Ω_{ci}	[-]	0.75	Relative stress level at start of non-linear hardening in compression
Ω_{cr}	[-]	0.10	Residual relative stress level in compression
G_{fc}	[Nm/m^2]	1000.0	Specific fracture energy in compression
G_{ft}	[Nm/m^2]	100.0	Specific fracture energy in tension
Ω_{tr}	[-]	0.05	Residual relative stress level in tension

3.3 Boundary Conditions

One of the aspects having a direct effect on the quality and solvability at all are the boundary conditions. At idealization of the solved problem in the ANSYS computational system the selected deformation load was set as the horizontal displacement on the boundary nodes of the mesh. In the first case study the zero vertical displacement was further specified on the boundary nodes on the right only to ensure a correct support of the model. However, considering the results this support appeared to be incorrect, which resulted in a change of the boundary conditions in the second case study. In this set of the computations, the zero vertical displacement was specified on the boundary nodes on the both sides of the sample. This arrangement of the boundary conditions had a positive effect on the quality of the results and so it was applied on the computational models in the third and fourth case study. The mentioned fourth and the last case study was already executed from the 3-D solid elements SOLID185 and therefore it requested a support in the horizontal and transverse direction. Considering the above-mentioned information this support was also carried out in the same manner as in the case of the vertical one. The consecutive idealization of the boundary conditions as it has been described above is documented in Fig. 5.

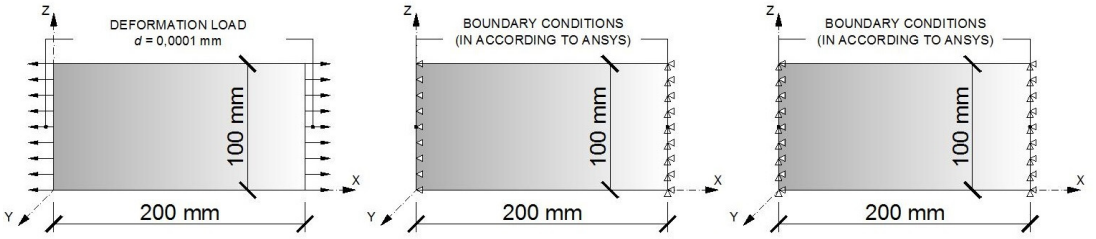

Fig. 5: Idealization of the boundary conditions

3.4 Results and Monitored Aspects

With regard to the complications occurred in the area of the idealization of the boundary conditions and the need to verify the correct functioning of the selected finite elements PLANE182 and SOLID185 4 sets of the case simulations in total were solved using the solver of the Newton-Raphson system of non-linear equations of the ANSYS computational system. Within these case studies, the effect of the different finite element mesh size of 1 mm, 2 mm, 5 mm, 10 mm and 20 mm was monitored.

The first set of the non-linear simulations using the above-mentioned material model with the vertical support of the computational model showed the incorrect results within the obtained *F-d* diagrams on one side only. Each of the curves had a different shape both in the area of the maximum tensile endurance, thus in the area of the localization of cracks, and at the descending branch. No connection with the dependence on the mesh was evident from the shapes of these curves and also from the values of the maximum tensile force $F_{t,\max}$ achieved, which are documented in Fig. 7(a). With respect to these results that are presented in Fig. 6(a), 7(a), 8(a), the boundary conditions were modified and subsequently a new set of the computational models was analysed.

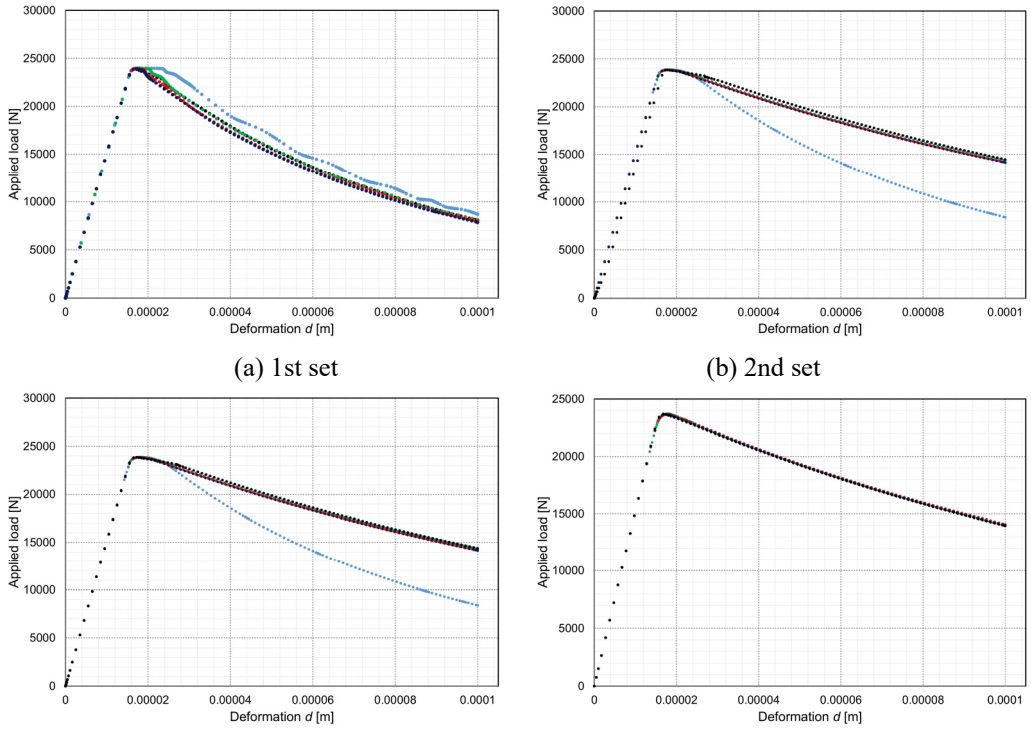

(a) 1st set (b) 2nd set

(c) 3rd set (d) 4th set

Fig. 6: *F-d* diagrams of solved case studies (— 1 mm, — 2 mm, — 5 mm, — 10 mm, — 20 mm)

In this second set of the simulations the previous irregularities were adjusted. However, the resulting *F-d* diagram of the computational model with the finite element mesh of the size of 1 mm diverged noticeably from the others. The shape of the resulting curves is shown in Fig. 6(b). The above-mentioned problems led to the adjustment of the internal variable of the PLANE182 element, where an enhanced strain formulation was chosen instead of the full integration. The 3rd set of the computational models of the virtual tension test was computed with the given modification at the level of the applied finite element. The results of the 3rd set are presented by Fig. 6(c), 7(c) and 8(c).

The last set of the numerical simulations was already executed on the 3-D solid elements SOLID185 that dispose of 3 translation degrees of freedom in all 8 nodes. The computations on this set showed to be very demanding from the point of view of the requirements on the hardware and the computational time. Due to this fact the model with the mesh of the size of 1 mm currently has not been analysed successfully yet, thus the graphs in Fig. 6(d), 7(d) and 8(d) do not show such information capability. Still, we can say that the resulting *F-d* diagrams for the meshes of 2 mm, 5 mm, 10 mm, 20 mm have almost identical form as the curves of the 2nd and 3rd set computed on the PLANE182 elements.

The conclusions made in the previous paragraphs are also documented in the graphs in Fig. 7(a) to 7(d). The graphs represent the intensity of the maximum achieved force $F_{t,max}$. As it has already been mentioned, the adjustment of the boundary conditions led to the considerable solution stabilization and the values of the maximum tensile force showed falling tendency when enlarging the finite element mesh. The graph in Fig. 7(d) where the error at the mesh of 20 mm most probably occurred represents the exception to the rule. The author assumes that the given error at the SOLID185 elements was caused by their inappropriately chosen size to the task dimensions.

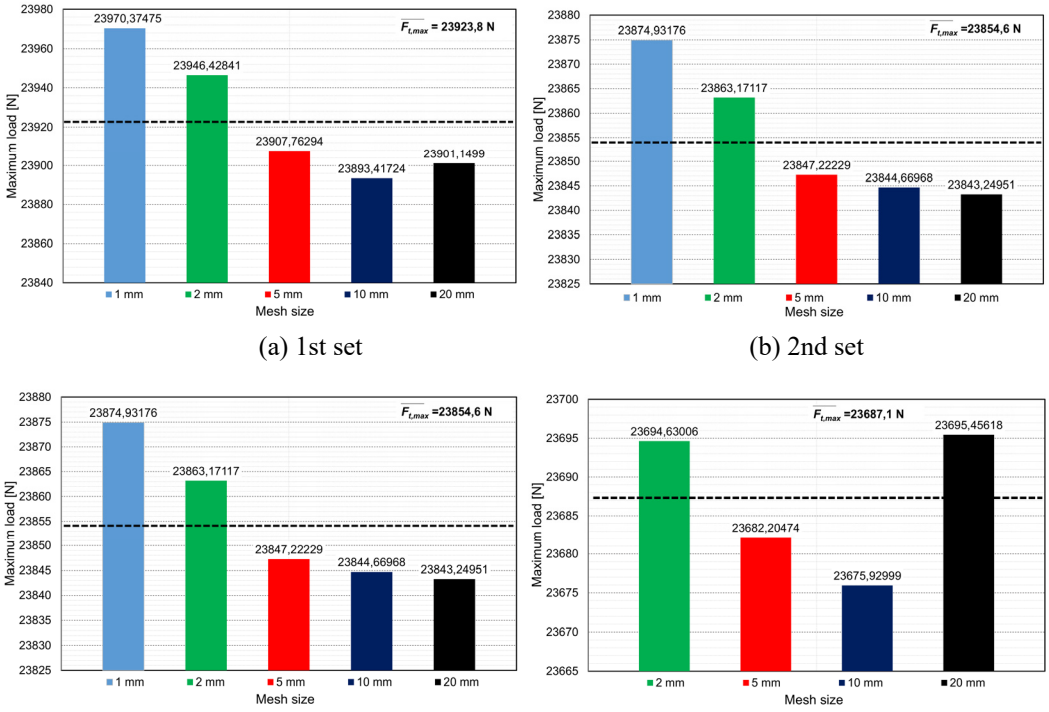

(a) 1st set (b) 2nd set

(c) 3rd set (d) 4th set

Fig. 7: $F_{t,max}$ diagrams of solved case studies
(— 1 mm, — 2 mm, — 5 mm, — 10 mm, — 20 mm)

When comparing the obtained results with the previously executed simplified analytic solution of the task we can state that there is a very good congruence between the computational and analytical solutions. The average intensity of the maximum achieved tensile force $F_{t,\max}$ reached 23.923 kN at the 1st set, 23.855 kN at the 2nd set, 23.855 kN at the 3rd set and 23.687 kN at the 4th set. There are thus deviations of 0.319 %; 0.606 %; 0.606 % and 1.304 %. Further we can mention that in the case of the 2nd and 3rd set the difference of the maximum tensile force $F_{t,\max}$ between 1 mm and 20 mm mesh reached the intensity of and $\Delta F_{t,\max,3}$ = 31.7 N. The above-mentioned values of the observed control variables and their comparison with the analytic solution is presented in Tab. 2.

Further, in Fig. 8(a) to 8(d) below the value of the initial tangential modulus of elasticity $E_{tan,ini}$ is presented. The accurate comparison of the achieved values including the deviations from the analytic solution is also summarize in Tab. 2.

Tab. 2: Calculated control variables and their comparison with the analytic solution

	$F_{t,max}$ [N]	$F_{t,max,avg}$ [N]	|Δ| [%]	E_c [GPa]	$E_{tan,ini,avg}$ [GPa]	|Δ| [%]
1st set	24000,0	23923.8	0.319	30.000	30.118	0.393
2nd set		23854.6	0.606		30.208	0.693
3rd set		23854.6	0.606		30.208	0.693
4th set		23687.1	1.321		30.402	1.322

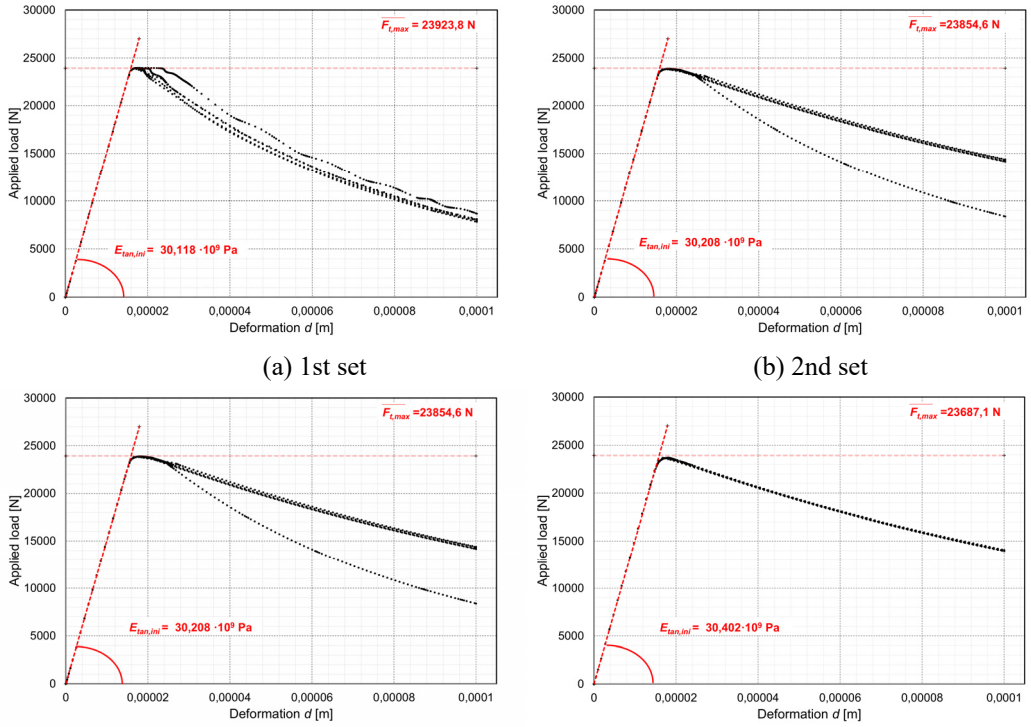

(a) 1st set (b) 2nd set

(c) 3rd set (d) 4th set

Fig. 8: Comparison of results

4 CONCLUSION

The published results of the numerical studies mapping the application of the multiPlas library of the material models prove the applicability of this computational tool for solution of the physically non-linear tasks. However, it should be mentioned, that the correct idealization of the specific task plays a significant role in the solving problems using the finite element method. In this respect the special attention has to be paid to the correct set of the boundary conditions. Although the selected problem was geometrically relatively simple, the negative dependence on the finite element mesh had an impact on some of the solved sets of the computation models.

This negative aspect proved at all the models with the mesh size of 1 mm. The results for the 2 mm mesh were already almost identical with 20 mm. Unfortunately, within the executed numerical case studies this negative aspect with the use of the 3-D solid elements SOLID185 failed to be proved or disproved, because of the hardware and time demandingness of the computation. However, the author believes that these results will be obtained successfully in the future.

ACKNOWLEDGMENT

The contribution has been created with the financial support of the project GACR 14-25320S "Aspects of the use of complex nonlinear material models" provided by the Czech Science Foundation and with financial support of the specific research project of Brno University of Technology FAST-J-14-2359 "Nonlinear computational models of prestressed concrete elements".

LITERATURE

[1] ANSYS INC. *ANSYS Mechanical APDL Theory Reference*. Canonsburg, PA 15317, 2013.

[2] ČERVENKA CONSULTING LTD. *ATENA Program Documentation*. Praha, 2013.

[3] BARTON D. C. Determination of the high strain rate fracture properties of ductile materials using a combined experimental/numerical approach. *International Journal of Impact Engineering* [online]. 2004, vol. 30, 8-9, pp. 1147-1159 [cit. 2015-11-29]. DOI: 10.1016/j.ijimpeng.2004.01.006. Available from: http://linkinghub.elsevier.com/retrieve/pii/S0734743X04000235.

[4] GRASSL, Peter and Milan JIRÁSEK. Damage-plastic model for concrete failure. *International Journal of Solids and Structures* [online]. 2006, vol. 43, 22-23, pp. 7166-7196 [cit. 2015-11-29]. DOI: 10.1016/j.ijsolstr.2006.06.032. Available from: http://linkinghub.elsevier.com/retrieve/pii/S002076830600240X.

[5] STRAUSS, Alfred, Thomas ZIMMERMANN, David LEHKÝ, Drahomír NOVÁK and Zbyněk KERŠNER. Stochastic fracture-mechanical parameters for the performance-based design of concrete structures. *Structural Concrete* [online]. 2014, vol. 15, issue 3, pp. 380-394 [cit. 2015-11-29]. DOI: 10.1002/suco.201300077. Available from: http://doi.wiley.com/10.1002/suco.201300077.

[6] HOKES, Filip. The Current State-of-the-Art in the Field of Material Models of Concrete and other Cementitious Composites. In: *Applied Mechanics and Materials* [online]. 2015, pp. 134-139 [cit. 2015-11-29]. ISSN 1662-7482. DOI: 10.4028/www.scientific.net/AMM.729.134. Available from: http://www.scientific.net/AMM.729.134.

[7] JIRÁSEK, Milan and Jan ZEMAN. *Deformation and failure of materials: creep, plasticity, fracture and damage. (Přetváření a porušování materiálů: dotvarování, plasticita, lom a poškození).* Vyd. 1. Praha: Nakladatelství ČVUT, 2006, 175 s. ISBN 978-80-01-03555-9.

[8] DYNARDO. *Multiplas: User's Manual Release 5.1.0 for 15.0*. Weimar, 2014.

[9] ČSN EN 1992-1-1. Eurocode 2: Design of concrete structures – Part 1-1: General rules and rules for buildings. Praha: ČNI, 2006.

[10] MENÉTREY, Philippe. *Numerical analysis of punching failure in reinforced concrete structures*. Lausane, 1994. PhD Thesis. EPFL.

[11] WILLAM K. J. and E. P. WARNKE. Constitutive models for the triaxial behavior of concrete. In *Proceedings of the International Association for Bridge and Structural Engineering*. 1975, vol. 9, pp. 1-30.

[12] BAŽANT, Zdeněk P. and B. H. OH. Crack band theory for fracture of concrete. *Matériaux et Constructions* [online]. 1983, vol. 16, issue 3, pp. 155-177 [cit. 2015-11-29]. DOI: 10.1007/BF02486267. Available from: http://link.springer.com/10.1007/BF02486267.

Reviewers:

Ing. Filip Fedorik, Ph.D., Structural Engineering and Construction Technology, University of Oulu, Finland.

Ing. Bc. Oldřich Sucharda, Ph.D., Department of Structural Mechanics, Faculty of Civil Engineering, VŠB – Technical University of Ostrava, Czech Republic.